HHS Public Access

Author manuscript

Immunity. Author manuscript; available in PMC 2017 May 17.

Published in final edited form as:

Immunity. 2016 May 17; 44(5): 1190–1203. doi:10.1016/j.immuni.2016.04.015.

PSGL-1 is an immune checkpoint regulator that promotes T cell exhaustion

Roberto Tinoco[1,2], **Florent Carrette**[1], **Monique L. Barraza**[1], **Dennis C. Otero**[1], **Jonathan Magaña**[1], **Marcus W. Bosenberg**[3], **Susan L. Swain**[4], and **Linda M. Bradley**[1]

[1]Infectious and Inflammatory Disease Center and NCI Designated Cancer Center, Sanford Burnham Prebys Medical Discovery Research Institute, La Jolla, CA 92037, USA

[2]Division of Biological Sciences, University of California, San Diego, La Jolla, CA 92093, USA

[3]Department of Pathology, Yale School of Medicine, New Haven, CT 06520, USA

[4]Department of Pathology, University of Massachusetts Medical School, Worcester, MA 01605, USA

Summary

Chronic viruses and cancers thwart immune responses in humans by inducing T cell dysfunction. Using a murine chronic virus that models human infections, we investigated the function of the adhesion molecule, P-selectin glycoprotein ligand-1 (PSGL-1) that is upregulated on responding T cells. PSGL-1-deficient mice cleared the virus due to increased intrinsic survival of multifunctional effector T cells that had downregulated PD-1 as well as other inhibitory receptors. Notably, this response resulted in $CD4^+$ T cell-dependent immunopathology. Mechanistically, PSGL-1 ligation on exhausted $CD8^+$ T cells inhibited T cell receptor (TCR) and interleukin-2 (IL-2) signaling, and upregulated PD-1, leading to diminished survival with TCR stimulation. In models of melanoma cancer where T cell dysfunction occurs, PSGL-1-deficiency led to PD-1 downregulation, improved T cell responses, and tumor control. Thus, PSGL-1 plays a fundamental role in balancing viral control and immunopathology, and also functions to regulate T cell responses in the tumor microenvironment.

Abstract

Contact: lbradley@sbpdiscovery.org

Author Contributions: R.T. initiated and designed the study and did the experiments with assistance from F.C., M.L.B., D.C.O., J.M. in the laboratory of L.M.B. S.L.S. provided critical input for experimental directions, expertise, and reagents. M.W.B. provided input, expertise, and reagents for the melanoma studies. R.T. analyzed, and together with L.M.B. interpreted experiments. R.T. and L.M.B. wrote the manuscript; and F.C. and S.L.S. provided advice and suggestions for the manuscript.

Competing Interests Statement: The authors declare that they have no competing financial interests.

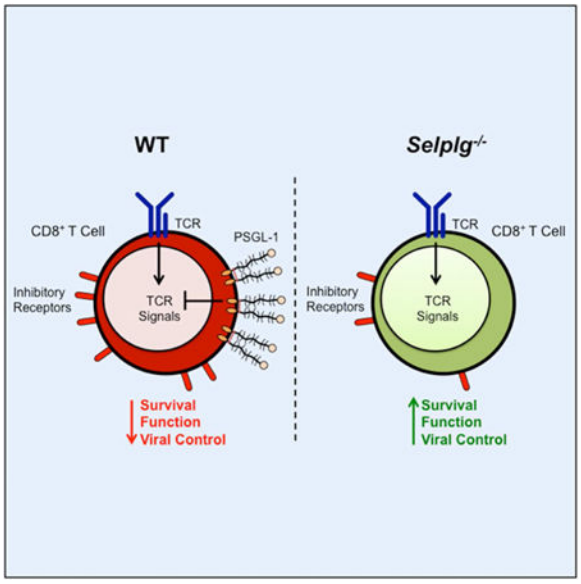

Keywords

Lymphocytic choriomeningitis virus Clone 13; P-selectin glycoprotein ligand-1; Programmed Death-1; T cell exhaustion; Immunopathology; Inhibitory Receptors; Melanoma; Cancer

Introduction

Immune responses by T lymphocytes mediate host protection against microbes, but they can become dysfunctional in chronic infections. With infections by viruses that become chronic, such as HIV and hepatitis B and C, T cells progressively lose responsiveness with elimination of many T cells by apoptosis and arrest of surviving T cells in a functionally impaired, exhausted state. A loss of T cell responsiveness can also develop in the context of cancer and thwart effective immune control. Although T cell exhaustion is incompletely understood, several underlying mechanisms have been identified in the Clone 13 (Cl13) lymphocytic choriomeningitis virus (LCMV) chronic infection model. With this infection, virus-specific $CD8^+$ T cells are chronically exposed to antigen (Shin et al., 2007) and they upregulate immune inhibitory receptors including PD-1, LAG3, CD160, and BTLA (Barber et al., 2006; Blackburn et al., 2009). They also lose motility (Zinselmeyer et al., 2013), show altered transcriptional regulation (Kao et al., 2011), and produce more of the inhibitory cytokines, interleukin-10 (IL-10) (Brooks et al., 2008) and transforming growth factor-β (TGF-β) (Tinoco et al., 2009). With time, $CD8^+$ T cells lose proliferative potential, cytotoxic function and ability to produce effector cytokines (Wherry, 2011). $CD4^+$ T cells also upregulate inhibitory receptors and lose function (Matloubian et al., 1994). Importantly, provision of functional virus-specific $CD4^+$ T cells can rescue exhausted $CD8^+$ T cells, enabling them to mediate viral clearance (Aubert et al., 2011). Therefore an interplay of several processes combine to disable the immune system's ability to eliminate chronic viral infections, and these may also contribute to inhibition of anti-tumor immunity.

It is now evident that in some cases, reversing T cell dysfunction can reestablish immune responses and achieve disease resolution against chronic viral infections (Brooks et al., 2006; West et al., 2013). This is also evident in immunotherapies to cancers where exhausted anti-tumor T cells are reinvigorated after inhibitory receptor blockade to eradicate tumors (Topalian et al., 2012). In the present study, we observed that PSGL-1, a ligand for the selectin family of receptors L, E, and P, was highly expressed on T cells after chronic LCMV Cl13 infection. Although, PSGL-1 is known for regulating T cell trafficking into inflamed tissues (Haddad et al., 2003) and into lymphoid tissues under steady-state conditions (Veerman et al., 2007), it may have additional potential function(s) during T cell responses to infections. $CD4^+$ T cells from *Selplg*$^{-/-}$mice cause exacerbated inflammation in a colitis model (Matsumoto et al., 2009) and *Selplg*$^{-/-}$ $CD8^+$ T cells undergo enhanced proliferation in lymphopenic hosts, and in response to IL-2 *in vitro* (Veerman et al., 2012). These findings imply a role for PSGL-1 in limiting T cell responses.

To test this prediction, we analyzed T cell responses to Cl13 in wild type (WT) and *Selplg*$^{-/-}$ mice. Although PSGL-1-deficiency did not alter initial T cell responses, T cell accumulation in lymphoid and nonlymphoid tissues was markedly increased due to cell-intrinsic enhanced survival along with preservation of multifunctional $CD4^+$ and $CD8^+$ T cell effectors with diminished expression of several immune inhibitory receptors that enabled viral clearance. This was accompanied by high serum concentrations of proinflammatory cytokines and pathology coupled with high mortality. This immunopathology in *Selplg*$^{-/-}$ mice was prevented by $CD4^+$ T cell depletion, which also abolished an effective $CD8^+$ T cell response. Further, PSGL-1 ligation on exhausted $CD8^+$ T cells in the context of TCR stimulation extinguished TCR signaling, promoted higher PD-1 expression, inhibited IL-2 signaling, and diminished their survival. Deficiency of PSGL-1 also prevented the development of T cell exhaustion by anti-tumor T cells in aggressive melanoma (Dankort et al., 2009), resulting in greatly reduced tumor growth. Thus we have uncovered a critical role for PSGL-1 in regulating $CD8^+$ T cell responses that is $CD4^+$ T cell-dependent and functions to restrain T cell responses.

Results

PSGL-1-Deficiency In Mice Leads to an accumulation of Virus-Specific T Cells after LCMV Cl13 Infection

To study PSGL-1 function we used LCMV Cl13, which causes prolonged viremia to 90-days post infection (dpi) with virus detectable in brain and kidneys to 200-dpi (Zajac et al., 1998). We first examined PSGL-1 on $CD8^+$ T cells specific for the $GP_{33\text{-}41}{}^+$ LCMV epitope. Although PSGL-1 is expressed by all T cells, expression was increased on virus-specific $CD8^+$ T cells in spleen, lymph node, and lung during infection, implying a possible role in regulating the response to Cl13 (Figure 1A,B). To examine contributions of PSGL-1 to the anti-viral response, we analyzed tetramer$^+$ $CD8^+$ T cells after infection of WT or *Selplg*$^{-/-}$ mice with Cl13. *Selplg*$^{-/-}$ mice had greatly increased frequencies and numbers of $GP_{33\text{-}41}{}^+$ and $NP_{396\text{-}404}{}^+$ $CD8^+$T cells at 8-dpi (Figure 1C,D). These differences were detected after 4-dpi (Figure S1A-C) and sustained through 30-dpi in spleen (Figure 1E) and blood (Figure S1D,E). We also observed preservation of $NP_{396\text{-}404}{}^+$ T cells (Figure 1C-H) that were

largely eliminated in WT mice. Since ligation of PSGL-1 on T cells by endothelial selectins can regulate migration into sites of inflammation (Ley et al., 2007), T cell accumulation in blood and spleen of *Selplg*$^{-/-}$ mice could reflect impaired entry into peripheral sites. Thus, we examined T cells in the lungs, a site of infection that unlike the spleen, requires adhesion receptor regulation for T cell entry. We observed greater accumulation of virus-specific CD8^{+} T cells (Figure 1F, S2A,B) in lungs of *Selplg*$^{-/-}$ than WT mice as well as in the liver (Figure 1G) and kidneys (Figure 1H). In addition, we found increased frequencies and numbers of LCMV-specific GP$_{66\text{-}76}$$^{+}$CD4^{+} T cells in *Selplg*$^{-/-}$ mice in spleen (Figure 1I,J) and lungs (Figure 1K, S2C,D). The results show that virus-specific T cells are preserved in higher numbers than WT cells in *Selplg*$^{-/-}$ mice.

Selplg$^{-/-}$ CD8^{+} T Cells Have Enhanced Survival and Reduced Inhibitory Receptor Expression

Enhanced expansion, survival or both could account for greater accumulation of virus-specific T cells in *Selplg*$^{-/-}$ mice. To assess proliferation we analyzed *in vivo* BrdU incorporation by GP$_{33\text{-}41}$$^{+}$CD8^{+} and GP$_{66\text{-}76}$$^{+}$CD4^{+} T cells at 8-dpi (Figure 2A,B). BrdU labeled 2x more WT cells than *Selplg*$^{-/-}$ cells, implying that division did not account for greater numbers of *Selplg*$^{-/-}$ T cells. Therefore, we examined expression of survival molecules by CD8^{+} T cells. Both GP$_{33\text{-}41}$$^{+}$ and NP$_{396\text{-}404}$$^{+}$ *Selplg*$^{-/-}$ T cells displayed increased IL-7Rα compared to WT cells from the time of virus-specific CD8^{+} T cell detection to 30-dpi (Figure 2C, S3A), implying an early and prolonged survival impact of PSGL-1 on T cells responding to Cl13. CD25 expression on GP$_{33\text{-}41}$$^{+}$ and NP$_{396\text{-}404}$$^{+}$ T cells from *Selplg*$^{-/-}$ mice were also increased (Figure 2D), whereas receptors for other cytokines that can regulate T cell survival were similar or reduced (Figure S2E-G). To directly measure apoptosis, we examined active Caspase3 and found fewer PI^{+}Caspase3^{+} CD8^{+} T cells in *Selplg*$^{-/-}$ mice than in WT mice (Figure 2E,F). Together, these findings indicate that the accumulation of virus-specific CD8^{+} T cells in *Selplg*$^{-/-}$mice results from enhanced survival and not hyper proliferation.

Since T cell exhaustion is linked to expression of multiple inhibitory molecules including PD-1, CD160, and BTLA (Blackburn et al., 2009), that can inhibit survival (Petrovas et al., 2006), we examined these receptors on virus-specific T cells. *Selplg*$^{-/-}$CD8^{+} T cells expressed lower PD-1, and similar expression of CD160 and BTLA at 8-dpi (Figure S3B,C), but all three receptors were decreased by 9-dpi (Figure 2G,H). Furthermore, *Selplg*$^{-/-}$ CD8^{+} T cells expressed reduced numbers of inhibitory receptors (PD-1, LAG3, TIM3) than WT cells (Figure 2I), and PD-1 downregulation was sustained to 112-dpi (Figure S3D). Inhibitory receptor downregulation on virus-specific CD8^{+} T cells was not only evident in the spleen (Figure S3E) but also in the kidneys and livers at 10-dpi (Figure S3F,G). We also found that PD-1 and BTLA expression on virus-specific GP$_{66\text{-}76}$$^{+}$ CD4^{+} T cells in *Selplg*$^{-/-}$ mice were also decreased at 8-dpi (Figure 2J). Consistent with PD-1 downregulation, CD8^{+} and CD4^{+} *Selplg*$^{-/-}$ T cells had reduced PD-1 signaling as indicated by decreased phospho-SHP2 (Sheppard et al., 2004) (Figure 2K,L).

We next determined the transcriptome of sorted GP$_{33\text{-}41}$$^{+}$ CD8^{+} T cells from WT and *Selplg*$^{-/-}$ mice at 9-dpi using RNAseq analysis. The data showed that WT GP$_{33\text{-}41}$$^{+}$ cells had

increased expression of genes associated with cell proliferation (*Ccdc28b*, *Mki67*,*Timp2*, *Kif15*), inhibitory receptors (*Cd160*, *Lag3*, *Tnfrsf9*, *Cd200*, *Pdcd1*), and cell death (*Bcl2l11*, *Casp3*). In contrast, *Selplg*$^{-/-}$ cells had increased expression of pro-survival genes (*Aqp9*, *Il6ra*, *Crem*, *Nr4a1*, *Il7r*). In addition, *Nfatc1*, which regulates inhibitory receptor expression, was also reduced in *Selplg*$^{-/-}$ cells (Martinez et al., 2015). *Nr4a1* (NUR77) which indicates TCR signaling (Baldwin and Hogquist, 2007) was increased in *Selplg*$^{-/-}$ T cells (Figure 2M). These findings demonstrate that virus-specific T cells in *Selplg*$^{-/-}$ mice had reduced expression and numbers of inhibitory receptors, reduced PD-1 signaling, and a transcriptome that favored their survival and responses after infection.

Virus-Specific T Cells in *Selplg*$^{-/-}$ Mice are Multifunctional Effectors

CD8^{+} T cell transcriptional programs become dysregulated after Cl13 infection and can be characterized by high Eomes and reduced T-bet expression that marks the most terminally differentiated effectors (Paley et al., 2012). Eomes expression was reduced in $GP_{33\text{-}41}{}^{+}$ and $NP_{396\text{-}404}{}^{+}$CD8^{+} T cells from *Selplg*$^{-/-}$ mice (Figure 3A) and T-bet was increased in $NP_{396\text{-}404}{}^{+}$CD8^{+} T cells (Figure 3B). Furthermore, *Selplg*$^{-/-}$ CD8^{+} T cells had reduced frequencies of Eomes^{hi} PD-1^{hi} cells (Figure 3C).

Cl13-induced T cell exhaustion is characterized by sequential loss of IL-2, TNF-α, and IFN-γ production by T cells (Moskophidis et al., 1993; Wherry et al., 2003; Zajac et al., 1998). We found that in *Selplg*$^{-/-}$ mice, Cl13 induced much higher frequencies of $GP_{33\text{-}41}{}^{+}$ (Figure 3D) and $NP_{396\text{-}404}{}^{+}$ T cells (Figure 3E) secreting IFN-γ, and both IFN-γ and TNF-α than in WT mice. Furthermore, virus-specific *Selplg*$^{-/-}$ CD8^{+} T cells had more CD107a^{+} IFN-γ^{+} cells, indicating they were undergoing better cytotoxic degranulation *in vivo* (Figure 3F). No differences in granzyme B (Gzmb) protein were seen (Figure 3G). Thus, while CD8^{+} T cells in WT mice develop exhaustion during Cl13 infection, in *Selplg*$^{-/-}$ mice they instead generated multifunctional effectors. *Selplg*$^{-/-}$ $GP_{66\text{-}76}{}^{+}$ CD4^{+} cells also had superior function (Figure 3H). Not only did more virus-specific CD4^{+} T cells from *Selplg*$^{-/-}$ mice produce IFN-γ, TNF-α, and IL-2 compared to WT cells, these were also multifunctional with more double and triple cytokine producers. The results demonstrate that like CD8^{+} T cells, greater numbers of functionally superior CD4^{+} T effectors develop in *Selplg*$^{-/-}$ mice after Cl13 infection.

Selplg$^{-/-}$ T Cells Are Not Hyperactivated in Uninfected Mice

To address whether phenotypic differences could account for the enhanced T cell response in *Selplg*$^{-/-}$ mice to Cl13 infection we characterized T cells from uninfected mice. For WT and *Selplg*$^{-/-}$ TCR transgenic P14^{+} cells, there were minor differences in CD44, CD62L, CD25, CD69, and IL-7Rα expression (Figure S4A,B). We found comparable T cell cellularity in 6-week or 6-month old WT and *Selplg*$^{-/-}$ mice (Figure S5A,B) with no differences in CD44 expression by CD4^{+} T cells but a 10% increase by CD8^{+} T cells (Figure S5C). No differences in T regulatory (Treg) cell frequencies, numbers, or capacity to inhibit proliferation of WT T cells were found (not shown); and *Selplg*$^{-/-}$ mice had a normal lifespan. We did not find differences in the serum concentrations of the pro-inflammatory cytokines IL-6, TNF-α, and IFN-γ (Figure S5D). or in IFN-γ production by *Selplg*$^{-/-}$ CD4^{+}

and CD8$^+$ T cells, although TNF-α production was reduced compared to WT cells (Figure S5E,F). These findings show that *Selplg*$^{-/-}$ T cells are not hyperactivated.

Accumulation of Virus-Specific *Selplg*$^{-/-}$ T Cells Is Cell-Intrinsic

To address what features of the improved response to Cl13 in *Selplg*$^{-/-}$ mice were T cell intrinsic, we transferred WT and *Selplg*$^{-/-}$ CD8$^+$ P14 cells or CD4$^+$ SMARTA cells, which recognize distinct LCMV epitopes, into WT mice. We cotransferred WT and *Selplg*$^{-/-}$cells at a 1:1 ratio and then infected with Cl13. We found increased numbers of *Selplg*$^{-/-}$P14 cells in spleen at 5- and 7-dpi (Figure 4A), and lungs (Figure S4C) with no differences in proliferation as measured by BrdU uptake at 8-dpi (not shown) and 13-dpi (Figure S4D,E). *Selplg*$^{-/-}$ SMARTA cells also accumulated to greater numbers than WT (Figure 4B). CFSE dilution in WT and *Selplg*$^{-/-}$ P14 cells was also comparable at 2-dpi (Figure 4C). Although we observed early increases in the numbers of P14 *Selplg*$^{-/-}$ T cells, they eventually became functionally exhausted and their numbers stabilized to WT T cells by 35-dpi (Figure 4D). These results indicate that CD8$^+$ and CD4$^+$ T cell survival is improved in the absence of PSGL-1.

PSGL-1 Ligation Decreases Survival of Exhausted CD8$^+$ T Cells with Upregulation of PD-1

To directly address the impact of PSGL-1 ligation on virus-specific CD8$^+$ T cells, we isolated splenocytes from WT mice at 9-dpi when CD8$^+$ T cells are functionally exhausted. After 4-days of *ex vivo* stimulation with GP_{33-41} peptide and IL-2 in the presence of anti-PSGL-1 antibody (clone 4RA10), the survival of tetramer$^+$ CD8$^+$ T cells decreased to those in cultures with media containing only IgG or anti-PSGL-1 (Figure 4E). PD-1 expression was sustained by peptide stimulation and was further elevated when anti-PSGL-1 was present (Figure 4F). Since IL-2 can rescue PD-1 inhibition and deliver pro-survival signals (Bennett et al., 2003), we addressed whether IL-2 signaling was affected by PSGL-1 ligation by analyzing pSTAT5 at 4-days after incubation with GP_{33-41} peptide, IL-2 and anti-PSGL-1. We found that in addition to increasing PD-1 (Figure 4F), PSGL-1 ligation reduced the frequencies of pSTAT-5$^+$ CD8$^+$ T cells (Figure 4G). These results show that PSGL-1 engagement during antigen stimulation limits the survival of CD8$^+$ T cells, sustains PD-1 expression and links PD-1, TCR and IL-2 signaling events to PSGL-1.

PSGL-1 Ligation Silences TCR Signaling in Exhausted CD8$^+$ T Cells and Further Increases Their Terminal Exhaustion Phenotype

PD-1 ligation can dampen TCR signals (Keir et al., 2008); to determine whether PSGL-1 could also impact TCR signaling in exhausted T cells, we purified responding CD8$^+$ T cells at 8-dpi and stimulated these cells with anti-CD3 and with control IgG or anti-PSGL-1. We examined phosphorylation of ERK1,2 (p-p44/42) and AKT (p-AKT^{S473}), two major TCR signaling pathways that regulate T cell function (Sabbagh et al., 2008; Sullivan et al., 2012). Immunoblot analysis showed that by 15 min, both IgG or anti-PSGL-1 treated WT cells induced p-ERK1,2 and p-AKT (Figure 4H). PSGL-1-ligation however, did not induce the maximal signal observed with IgG-treated cells by 15 or 30 minutes, and these downstream TCR signals were extinguished by 2-hrs (Figure 4H). In contrast, *Selplg*$^{-/-}$ CD8$^+$ T cells treated with IgG or anti-PSGL-1 had robust p-ERK1,2 and p-AKT signals at 2-hrs (Figure 4H). Two additional clones of anti-mouse PSGL-1 antibodies clones 2PH1 (Borges et al.,

1997) and 4RB12 (Engelhardt et al., 2005) did not affect TCR signaling or PD-1 expression *in vitro* (not shown).

We next explored whether blocking the major known receptors for PSGL-1, all three selectins, or ligating PSGL-1 *in vivo* could impact T cell exhaustion. Treatment with anti-P-selectin, anti-E-selectin, and anti-L-selectin did not alter the frequencies of GP_{33-41}^+ or $NP_{396-404}^+$ cells at 8-dpi (Figure 4I, S6A). While the anti-PSGL-1 antibodies, 2PH1 and 4RB12, did not affect T cell responses to Cl13 (not shown), treatment with 4RA10 anti-PSGL-1 decreased the frequency of virus-specific $CD8^+$ T cells (Figure 4I, S6A) and resulted in increased LAG3 and TIM3 expression compared to IgG or anti-P,-E,-L treated animals (Figure S6B,C). In addition, ligating PSGL-1 increased the number of inhibitory receptors (PD-1, LAG3, TIM3) expressed by virus-specific $CD8^+$ T cells (Figure S6D). Viremia was similar in all three groups at 36-dpi (Figure S6E). Since additional studies showed CCL19 and CCL21 binding to PSGL-1 (Carlow et al., 2009), we tested whether their absence could improve the expansion of WT P14 cells to those of *Selplg*$^{-/-}$ P14 cells in *plt* mice that lack these chemokines (Nakano and Gunn, 2001) and found no effect on their expansion or PD-1 expression (Figure S6F,G). These findings demonstrate that PSGL-1 can negatively regulate TCR signaling, increase inhibitory receptor expression, and limit the frequencies of virus-specific $CD8^+$ T cells, thus exacerbating T cell exhaustion.

Selplg$^{-/-}$ Mice Clear Chronic LCMV But Develop Enhanced Immunopathology

Since we observed improved T cell functionality in *Selplg*$^{-/-}$ mice, we examined viral control. WT mice had elevated viremia at 30-dpi, while *Selplg*$^{-/-}$ mice showed viral clearance by 15-dpi in blood (Figure 5A) and 30-dpi in liver (Figure 5B) and kidney (Figure 5C). However, heightened T cell responses resulted in greater than 50% mortality from 8-dpi onwards (Figure 5D). Furthermore, PSGL-1-deficiency was associated with elevated circulating concentrations of the proinflammatory cytokines, IL-6, IL-21, TNF-α, and IFN-γ (Figure 5E). In addition, in the lungs, infiltrates (Figure 5F), edema, and inflammation were increased (Figure 5G). Elevated pathology was also evident in livers (Figure 5G). We found that *Selplg*$^{-/-}$ mice had similar frequencies and numbers of Tregs at 9-dpi (not shown). All *Selplg*$^{-/-}$ mice survived when infected with acute LCMV Armstrong infection (not shown). Thus, although *Selplg*$^{-/-}$ mice controlled chronic viral replication much more effectively than WT mice, this resulted in extensive inflammation and increased mortality due to immunopathology.

Optimal Virus-Specific $CD8^+$ T Cell Function In *Selplg*$^{-/-}$ Mice Requires $CD4^+$ T Cells

Since we observed increases in the numbers and functionality of GP_{66-76}^+ $CD4^+$ T cells in *Selplg*$^{-/-}$ mice (Figure 6A), we examined whether they contribute to the effective anti-viral response by administering a depleting antibody. When we compared the responses of WT and *Selplg*$^{-/-}$ $CD8^+$ T cells with or without $CD4^+$ T cells, we found that $CD4^+$ T cell-depleted *Selplg*$^{-/-}$ mice had reduced frequencies of GP_{33-41}^+ and $NP_{396-404}^+$ $CD8^+$ T cells, approximating those found in WT mice (Figure 6B). The depletion of $CD4^+$ T cells also resulted in reduced numbers of IFN-γ^+ and IFN-γ^+TNF-α^+ $CD8^+$ T cells (Figure 6C) and this was mirrored by changes in PD-1 on GP_{33-41}^+ and $NP_{396-404}^+$ T cells, which remained elevated and similar to WT cells (Figure 6D). Unlike *Selplg*$^{-/-}$ mice in which serum Cl13

titers were reduced at 10-dpi, viremia in $CD4^+$ T cell-depleted mice remained comparable to that observed in WT mice (Figure 6E). Furthermore, the enhanced mortality of *Selplg*$^{-/-}$ mice was abolished (Figure 6E). We conclude that $CD4^+$ T cell help is required to support the changes in virus-specific $CD8^+$ T cells what occur with PSGL-1-deficiency.

PSGL-1 Limits Anti-Tumor T Cell Function Facilitating Melanoma Tumor Growth

Effector T cell dysfunction is widely documented in the setting of anti-tumor immunity (Gajewski et al., 2013). Treatments with mAbs that interfere with engagement of the PD-1 and PD-L1 and/or CTLA-4 and B7 pathways can greatly improve anti-tumor T cell responses, notably in malignant melanoma (Wolchok et al., 2013). To address whether T cell dysfunction could be influenced by PSGL-1 in this setting, we analyzed tumors of a melanoma cell line (Yumm1.5) derived from a primary tumor from an inducible melanoma model that recapitulates many aspects of the human disease (Dankort et al., 2009). In this model, induction of the $BRAF^{V600E}$ mutation found in ∼65% of skin cancer patients is combined with deletion of *Pten* and *Cdkn2a* (Chin, 2003; Lin et al., 2008). We injected tumor cells s.c. into WT or *Selplg*$^{-/-}$ mice and monitored their growth. There was better tumor control in *Selplg*$^{-/-}$ mice than in WT mice (Figure 7A), as indicated by slower growth. Furthermore, ∼18-20% of *Selplg*$^{-/-}$ mice were tumor free whereas all WT mice had tumors.

Tumor-infiltrating $CD44^{hi}$ effector $CD8^+$ and $CD4^+$ T cells were significantly increased in *Selplg*$^{-/-}$ mice compared to WT mice (Figure 7B,D). In addition, PD-1 expression on both $CD4^+$ and $CD8^+$ T cells in *Selplg*$^{-/-}$ mice was lower compared to WT cells (Figure 7C,E). We also detected increased frequencies of multifunctional $CD4^+$ and $CD8^+$ T cells that produced IFN-γ, TNF-α, and IL-2 compared to WT cells (Figure 7F-H). We did not detect differences in Treg numbers in tumors (Figure 7I). To determine the role of PSGL-1-deficiency in T cells in Yumm1.5 tumor control, $CD4^+$ and $CD8^+$ T cells were depleted from WT and *Selplg*$^{-/-}$ mice by antibody treatment. Tumor growth was identical in WT and *Selplg*$^{-/-}$ mice (Figure S7A,B), indicating T-cell dependence of the improved response.

To directly address the effect of PSGL-1 deficiency in $CD8^+$ T cells, we injected WT mice with B16 melanoma cells expressing OVA. WT or *Selplg*$^{-/-}$ OT-I TCR transgenic $CD8^+$ T cells specific for OVA were stimulated *in vitro* for 48-hrs and injected into WT mice 7-days after B16-OVA injection. *Selplg*$^{-/-}$ OT-I cells were more effective at delaying tumor growth (Figure 7J). However B16-OVA ultimately escaped the T cell response, suggesting that as with Cl13 infection, exhaustion can be reestablished. Together, these results indicated that a PSGL-1-dependent pathway in T cells inhibits the anti-tumor response against melanoma by diminishing their effector function, and in this context loss of PSGL-1 can improve T cell-mediated control.

Discussion

Chronic viral infections represent an altered state of homeostasis, an intricate balance between host and pathogen where both survive, albeit at the expense of host immune suppression. Although PSGL-1 is primarily known to regulate cell migration, its elevated expression on effector T cells and its signaling capacity raise the possibility of additional functions (Urzainqui et al., 2002; Zarbock et al., 2009). In this study, we have established

that PSGL-1 acts as a potent negative regulator of T cell function that can be exploited by a chronic virus to restrain effector T cells, thereby permitting a persistent infection, while also limiting immune-mediated host tissue damage. Our finding that PSLG-1 also restrains T cell responses in the context of tumors supports a conclusion that this receptor has broad potential to regulate the magnitude of immune responses.

During Cl13 infection, *Selplg*$^{-/-}$ hosts generated T cells that, in contrast to those of WT mice, failed to acquire hallmarks of exhaustion, and instead developed into robust multifunctional effectors that were maintained and promoted viral clearance. Both of these outcomes required CD4^{+} T cells. This effective anti-viral response was linked to reduced expression of inhibitory receptors on both CD8^{+} and CD4^{+} T cells. Mechanistically, ligating PSGL-1 on exhausted T cells in the context of TCR engagement extinguished ERK and AKT signaling, two major signaling pathways that regulate T cell survival and function. More limited TCR engagement *in vivo* was confirmed by decreased *Nur77* transcription in WT compared to *Selplg*$^{-/-}$ CD8^{+} T cells after Cl13 infection. We also found that PSGL-1 ligation upregulated PD-1 and reduced downstream IL-2 signaling to decrease survival. With melanoma tumors, we observed that PSGL-1 limits anti-tumor responses by promoting high PD-1 expression and loss of multifunctional effectors, and in its absence tumor control is improved. Together these results indicate that PSGL-1 functions as a key negative regulator of CD8^{+} and CD4^{+} T effector cells that limits the extent of their responses in the context of prolonged, chronic antigen exposure, attenuating their function and reducing their survival. In support of this conclusion, we find that T cells from *Selplg*$^{-/-}$ mice display better survival as effector and memory cells than WT even after infection with the LCMV Armstrong strain that is effectively cleared (not shown), suggesting that PSGL-1 can function generally to limit the magnitude of T cell responses.

Underscoring the functional changes in CD8^{+} T cells with PSGL-1-deficiency, we show prevention of transcriptional changes that are associated with CD8^{+} T cell dysfunction in response to Cl13 (Paley et al., 2012). We found decreased Eomes and increased T-bet expression, a program associated with effector T cell development. High T-bet can repress PD-1 expression (Kao et al., 2011), and we observed that PSGL-1 deficiency reciprocally regulated both molecules to support an improved effector T cell response. Furthermore, with Cl13 infection, PSGL-1 expression leads to inhibition of multiple genes associated with CD8^{+} T cell survival and function and upregulation of genes and transcription programs associated with terminal differentiation. The results underscore the conclusion that by attenuating TCR signaling, PSGL-1 is broadly linked to transcriptional changes that facilitate exhaustion.

We did not find selectins to be required as receptors for PSGL-1 during Cl13 infection, consistent with our finding that the majority of exhausted CD8^{+} T cells do not bind P-selectin (not shown). Furthermore, although CCL-19 and CCL-21 bind to PSGL-1 and potentially signal (Carlow et al., 2009), *plt* mice, which lack these chemokines (Nakano and Gunn, 2001), became persistently infected with Cl13 (not shown) and adoptively transferred WT P14 CD8^{+} T cells also became phenotypically exhausted. These results are supported by our finding that T cell migration into tissues does not require PSGL-1 and imply that additional binding partners can regulate PSGL-1 signaling during Cl13 infection.

A key impact of PSGL-1 deficiency was intrinsic T cell accumulation that was associated with increased and sustained expression of IL-7Rα and IL-2Rα and decreased apoptosis. These results suggest that enhanced responsiveness to IL-7 and IL-2 contribute to improved effector T cell survival and function. Indeed, therapeutic IL-7 administration in mice expands $CD8^+$ T cells, increases their effector function, and controls Cl13 infection (Pellegrini et al., 2011). Likewise, when administered to Cl13 infected mice, IL-2 also increases $CD8^+$ T cell responses and reduces viral loads (Blattman et al., 2003). Moreover, we have shown greater production of IL-2 by *Selplg*$^{-/-}$$CD4^+$ T cells, which would support $CD4^+$ and $CD8^+$ T cell survival and function. It is notable that ligating PSGL-1 on exhausted $CD8^+$ T cells with anti-PSGL-1 clone 4RA10 in combination with TCR engagement reduced IL-2 signaling via STAT-5 as well as their survival. Since TGF-β_1 apoptotic signals to $CD8^+$ T cells can be overcome by IL-2 and IL-7 (Sanjabi et al., 2009), responsiveness to these cytokines is likely to be critical for PSGL-1 mediated regulation of T cells after Cl13 infection. Although PSGL-1 was reported to limit proliferation of naïve $CD8^+$ T cells to IL-2 and IL-15 *in vitro* (Veerman et al., 2012), we did not observe greater proliferation of *Selplg*$^{-/-}$ virus-specific $CD8^+$ or $CD4^+$ T cells *in vivo* after Cl13 infection, suggesting that PSGL-1 does not impact clonal burst in this setting.

Since the maintenance of T cell dysfunction after chronic viral infections is associated with several immune inhibitory receptors (Blackburn et al., 2009; Virgin et al., 2009), it is striking that all of the receptors we analyzed (PD-1, CD160, BTLA, TIM3, LAG3) were down-modulated on *Selplg*$^{-/-}$ $CD8^+$ and $CD4^+$ effectors and this corresponded with dramatically improved anti-viral responses. Furthermore, since the frequency of $CD8^+$ T cells expressing multiple inhibitory receptors simultaneously was increased in WT mice, the results imply that PSGL-1 is normally a key part of a regulatory program that controls terminal differentiation of exhausted T cells. This conclusion is supported by our data showing dramatically improved cytokine responses of melanoma tumor infiltrating $CD4^+$ and $CD8^+$ T cells, reduced PD-1 expression and delayed tumor growth with PSGL-1 deficiency. However, since PSGL-1-deficiency does not lead to spontaneous inflammatory responses (Veerman et al., 2012), our finding of immunopathology, high serum concentrations of proinflammatory cytokines, and increased mortality after Cl13 infection underscores the function of PSGL-1 in controlling effector T cell responses after their induction. These outcomes are also found with PD-1-deficient mice after Cl13 infection. However, unlike in PD-1-deficient mice where 100% mortality occurs (Frebel et al., 2012), in *Selplg*$^{-/-}$ mice that survive and control Cl13 infection, virus-specific T cells persist and mice live a normal lifespan with no apparent signs of autoimmunity. Since PSGL-1 ligation attenuates TCR signals and leads to upregulation of PD-1 on exhausted $CD8^+$ T cells, PSGL-1 could act as a regulator of PD-1 expression. PSGL-1 signaling may also directly or indirectly contribute to regulation of additional pathways that lead to T cell exhaustion.

Our results reveal that the functionality of $CD8^+$ T cells in *Selplg*$^{-/-}$ mice requires $CD4^+$ T cells to realize the regulatory activity of PSGL-1. Our data also indicate that protracted antigen exposure, which are associated with chronic virus infection or the establishment of a tumor are necessary to reveal the profound PSGL-1-dependent inhibitory effects. Many hematopoietic cells express PSGL-1, including DCs and Treg cells on which it has been associated with functional regulation, delineating tolerogenic DCs and highly suppressive

Treg cells (Urzainqui et al., 2007). Therefore, PSGL-1 could play roles by altering other cells that indirectly contribute to T cell dysfunction during chronic infection, although we did not find changes in Treg cells or their function in *Selplg*$^{-/-}$ mice (not shown) or altered cellularity. Although trafficking of pre-T-cells to the thymus (Matsumoto et al., 2009), and of naïve CD4^{+} T cells to lymph nodes is altered in *Selplg*$^{-/-}$ mice (Veerman et al., 2007), peripheral naïve T cells appear to be generated normally, and memory phenotype cells are somewhat increased. Given the T cell intrinsic effects of PSGL-1-deficiency on effector cell survival and reversal of enhanced anti-viral immunity with CD4^{+} T cell depletion, more subtle aspects of regulation in context of PSGL-1-deficiency do not appear to make a substantive contribution to the outcomes of our study.

Recent clinical trials with anti-PD-1, PD-L1 and/or CTLA-4 (Topalian et al., 2012) support the concept that immunity to chronic virus or tumors can be improved by interfering with inhibitory pathways. Furthermore, targeting combinations of inhibitory receptors can lead to greater efficacy (Larkin et al., 2015). Since multiple inhibitory receptors are impacted by PSGL-1, this receptor could be a novel target for which a functional blockade could generally improve T cell responses in many clinical settings, including with tumors that are unresponsive to checkpoint inhibition, and with infections where T cell immune responses are suboptimal.

Experimental Procedures

Mice

C57BL/6J and *Selplg*$^{-/-}$ mice were purchased from the Jackson Laboratory, then bred in SPF facilities and maintained BSL-2 facilities after infection in the Institute's vivarium. *Selplg*$^{-/-}$ mice were backcrossed to C57BL/6J mice for more than 10 generations. P14 and SMARTA mice were from Charles D. Surh (La Jolla Institute for Allergy and Immunology). OT-I mice were from William R. Heath (University of Melbourne). These mice were bred to Ly5.1 (B6.SJL-Ptprc^{a} Pepc^{b}/BoyJ) mice and to Thy1.1 (B6.PL-Thy 1^{a}/CyJ), *Selplg*$^{-/-}$ mice. Both male and female mice were used at ≥6 weeks of age. All experiments were approved by the Institute's IACUC Committee.

Infection

LCMV Cl13 strain was propagated in baby hamster kidney cells and titrated on Vero African green monkey kidney cells. Frozen stocks were diluted in Vero cell media and 2×10^{6} plaque-forming units (PFU) of LCMV Cl13 were injected i.v.

Flow cytometry

For cell surface staining, 2×10^{6} cells were incubated with antibodies (see supplementary methods) in staining buffer (PBS, 2%FBS and 0.01%NaN_3) for 20 min at 4°C, and with H-2D ^{b}-GP_{33-41}, H-2D^{b}-$NP_{396-404}$ tetramers (Beckman Coulter) or IA^{b}-$_{66-77}$ tetramer (NIH core facility) for 1hr 15 min at room temperature. For Cl13 studies, the cells were cultured for 5 hr at 37°C with 2 μg/mL of GP_{33-41}, $NP_{396-404}$ and GP_{61-80} peptides (AnaSpec). For melanoma studies, WT and *Selplg*$^{-/-}$ cells from the tumors were incubated with three melanoma peptides (2μg/mL each), $gp100_{25-33}$, Melan-A_{26-35}, TRP-$2_{180-188}$, TRP-$2_{181-188}$

(AnaSpec), for 16hr at 37°C. CD4 $^{+}$ T cells were assessed after culture with PMA (10ng/mL) and Ionomycin (0.5μg/mL) for 5 hr at 37°C. The culture media was RPMI-1640 containing 10mM hepes, 1% non-essential amino acids and L-glutamine, 1mM sodium pyruvate, 10% heat-inactivated FBS and antibiotics (complete medium), that also included 50U/mL IL-2 (NCI), and 1μg/mL Brefeldin A (Sigma). The cells were then surface stained, fixed, permeablilized, and then stained for cytokines (protocol from BD Biosciences). For phosphoflow staining, cells were first stained with GP_{33-41} tetramer as above, then fixed with 1.85% formaldehyde in PBS for 7min at 37°C, followed by incubation in 90% methanol on ice for 30min. After washing, the cells were stained with pSTAT-5 antibody (BD clone 47) or mouse IgG1 platelet control g_1 (BD). Transcription factor staining (Eomes and T-bet) and detection of cleaved Caspase3 was performed using protocols from eBiosciences. All staining was done in 96 well plates. A LSRFortessa flow cytometer (BD) was used for analysis.

In vivo proliferation

Mice were injected i.p. with 2mg BrdU (Sigma-Aldrich) 16 hr before removing the spleens and lungs at 8- or 13-dpi. Proliferation of $CD8^+$ T cells from spleens of WT and *Selplg*$^{-/-}$ P14 mice was measured after negative enrichment (Stemcell Technologies), labeling with CFSE (5μM, Life Technologies) and coinjection of WT and *Selplg*$^{-/-}$ cells (1×10^6 cells of each) i.v. into WT mice that were infected one day later with Cl-13. CFSE-dilution was analyzed at 2-dpi.

PSGL-1 ligation

At 9-dpi, 2×10^6 splenocytes from WT mice were cultured for 96hr in complete medium supplemented 2-ME and 50 U/mL IL-2 under the following conditions: 10μg/mL rat IgG (Jackson ImmunoResearch), 10μg/mL anti-PSGL-1 (4RA10, BioXCell), 2μg/mL GP_{33-41} peptide or both anti-PSGL-1 and peptide. Cultured cells were tetramer stained and live cells determined by excluding PI^+ cells. For pSTAT-5 staining, cells were incubated with 5μg/mL of IgG or anti-PSGL-1 and stimulated with GP_{33-41} peptide as above. Additionally, responding $CD8^+$ T cells ($CD8^+CD44^+CD11a^+CD49d^+$) were FACS-sorted from spleens of CL13 infected mice at 9-dpi to >96% purity. The cells were stimulated for the indicated times with plate bound anti-CD3 (10μg/mL) and plate bound rat IgG or anti-PSGL-1 followed by immunoblotting with antibodies specific for phospho ERK1/2-Thr202/Tyr204, phospho AKT-Ser473, ERK1/2, and AKT (all from Cell Signaling Technologies).

In vivo antibody treatments

Mice were injected i.p. with 600μg IgG, or with 200μg anti-P-selectin (RME-1, Biolegend), 200μg anti-E-selectin (RMP-1, Biolegend) and 200μg anti-L-selectin (Mel-14, BioXcell), or 200μg anti-P-selectin and 200μg anti-PSGL-1 (4RA10) i.p. 0, 3-, and 5-dpi of WT mice with 2×10^6 Cl13. Viral titers in blood were determined at 8- and 36-dpi. To deplete $CD4^+$ cells, mice received two 500μg i.p. injections of anti-CD4 antibody (GK1.5, BioXCell) at day -1 and 0 with respect to Cl13 infection. Efficacy of CD4 depletion was confirmed in blood and spleens by flow cytometry.

Transcriptome analysis

At 9-dpi of WT or *Selplg*$^{-/-}$ mice, CD8^{+} T cells were negatively enriched from pooled spleen cells (10 mice per group), tetramer stained, and then live GP$_{33-41}$$^{+}$ CD8^{+} cells were FACS sorted to >98% purity (not shown). After RNA isolation (RNeasy Microkit-Qiagen) from 2 biological replicates, sequencing analysis was performed using the Illumina platform (Sanford Burnham Prebys Medical Discovery Institute, Lake Nona, FL). Data were analyzed using the following parameters: reference genome and transcript annotations from mm10 from UCSC; Mapping-TopHat splice-aware aligner; Expectation-Maximization (EM) approach use to estimate transcript abundance; Normalization within sample RPKM (reads per kilobase of transcript per million) and between sample TMM (Trimmed mean of M values); Differential test DE analysis with EdgeR software. Differentially expressed gene transcripts had criteria of at least one sample with RPKM over 1, Fold change over 2, and p-value ≤ 0.05. Analysis 1350 transcripts met these criteria; 578 transcripts were upregulated on WT while 772 were downregulated. The data are available in the Gene Expression Omnibus (GEO), accession GSE80113.

Cytokines and pathology

Sera from WT and *Selplg*$^{-/-}$ mice that were uninfected or infected with Cl13 8 days earlier were examined for concentrations of IL-6, IL-21, TNF-α, and IFN-γ using a multiplex 9-bead custom cytokine array (Millipore). Samples were analyzed with a Luminex IS200 instrument. Liver, kidney, and lungs were fixed in zinc formalin (z-fix Anatech), embedded in paraffin, and sectioned. Tissues were stained with H&E and digitally scanned using Aperio ScanScope. Pathology scoring was a blind assessment of tissue samples by a pathologist. Scores ranged from 0-3.5, with zero indicating no pathology and greater scores indicated increased pathology.

Melanoma Models

BRAF$^{V600E/+}$; *Pten*$^{-/-}$; *Cdkn2a*$^{-/-}$ mouse melanoma cells (Yumm1.5) were provided by Marcus Bosenberg (Yale University). Male WT or *Selplg*$^{-/-}$ mice were injected s.c. in the right flank with 5×10^3 cells for time points >1 month or with 5×10^5 cells for time points of 2 weeks. Tumor growth was measured using calipers. Tumors were excised, weighed, minced and collagenase digested for 1hr. Cells were passed through a 75μm strainer and then stained for flow cytometry. For the B16 melanoma model, WT mice were injected s.c. with 1×10^6 B16-OVA cells. WT OT-I or *Selplg*$^{-/-}$ OT-I T cells were stimulated with OVA$_{257-264}$ (2μg/mL) peptide in complete media with 50 U/mL IL-2 for 48hr, purified by negative selection, and 1×10^6 cells were separately injected i.v. at 7 days after tumor cell injection. Tumor growth was followed to day 10 post T cell injection.

Data Analysis

Flow cytometry data were analyzed with FlowJo software (TreeStar). Graphs were prepared using GraphPad Prism software. GraphPad Prism was used for statistical analysis to compare outcomes using a 2-tailed unpaired student *t* test; significance was set to $p<0.05$ and represented as *(<0.05), **(<0.005), ***(<0.001), **** (<0.001). Error bars show

SEM. A Mantel-Cox and Gehan-Breslow-Wilcoxon test was used to compare survival curves.

Supplementary Material

Refer to Web version on PubMed Central for supplementary material.

Acknowledgments

The authors thank Drs. Monica Macal, Robert Rickert and Carl Ware for critical review of the manuscript; Dr. Denise M. Malicki, UCSD Rady Children's Hospital for pathology analysis; and Miguel Reina Campos for assistance with RNAseq analysis. R.T is supported by NIH IRACDA K12 GM068524 Fellowship and UC San Diego Chancellor's Postdoctoral Fellowship. This work was supported by NIH grants P01-AI046530 to S.L.S and L.M.B. and R01-AI106895 and Melanoma Research Foundation grant 322189 to L.M.B. This work was also supported by NCI Cancer Center Grant P30 CA030199, which supports the animal, flow cytometry and histology cores at the La Jolla campus.

References

Aubert RD, Kamphorst AO, Sarkar S, Vezys V, Ha SJ, Barber DL, Ye L, Sharpe AH, Freeman GJ, Ahmed R. Antigen-specific CD4 T-cell help rescues exhausted CD8 T cells during chronic viral infection. Proc Natl Acad Sci U S A. 2011; 108:21182–21187. [PubMed: 22160724]

Baldwin TA, Hogquist KA. Transcriptional analysis of clonal deletion in vivo. J Immunol. 2007; 179:837–844. [PubMed: 17617574]

Barber DL, Wherry EJ, Masopust D, Zhu B, Allison JP, Sharpe AH, Freeman GJ, Ahmed R. Restoring function in exhausted CD8 T cells during chronic viral infection. Nature. 2006; 439:682–687. [PubMed: 16382236]

Bennett F, Luxenberg D, Ling V, Wang IM, Marquette K, Lowe D, Khan N, Veldman G, Jacobs KA, Valge-Archer VE, et al. Program death-1 engagement upon TCR activation has distinct effects on costimulation and cytokine-driven proliferation: attenuation of ICOS, IL-4, and IL-21, but not CD28, IL-7, and IL-15 responses. J Immunol. 2003; 170:711–718. [PubMed: 12517932]

Blackburn SD, Shin H, Haining WN, Zou T, Workman CJ, Polley A, Betts MR, Freeman GJ, Vignali DA, Wherry EJ. Coregulation of CD8+ T cell exhaustion by multiple inhibitory receptors during chronic viral infection. Nat Immunol. 2009; 10:29–37. [PubMed: 19043418]

Blattman JN, Grayson JM, Wherry EJ, Kaech SM, Smith KA, Ahmed R. Therapeutic use of IL-2 to enhance antiviral T-cell responses in vivo. Nat Med. 2003; 9:540–547. [PubMed: 12692546]

Borges E, Eytner R, Moll T, Steegmaier M, Campbell MA, Ley K, Mossmann H, Vestweber D. The P-selectin glycoprotein ligand-1 is important for recruitment of neutrophils into inflamed mouse peritoneum. Blood. 1997; 90:1934–1942. [PubMed: 9292527]

Brooks DG, Ha SJ, Elsaesser H, Sharpe AH, Freeman GJ, Oldstone MB. IL-10 and PD-L1 operate through distinct pathways to suppress T-cell activity during persistent viral infection. Proc Natl Acad Sci U S A. 2008; 105:20428–20433. [PubMed: 19075244]

Brooks DG, Trifilo MJ, Edelmann KH, Teyton L, McGavern DB, Oldstone MB. Interleukin-10 determines viral clearance or persistence in vivo. Nat Med. 2006; 12:1301–1309. [PubMed: 17041596]

Carlow DA, Gossens K, Naus S, Veerman KM, Seo W, Ziltener HJ. PSGL-1 function in immunity and steady state homeostasis. Immunol Rev. 2009; 230:75–96. [PubMed: 19594630]

Chin L. The genetics of malignant melanoma: lessons from mouse and man. Nat Rev Cancer. 2003; 3:559–570. [PubMed: 12894244]

Dankort D, Curley DP, Cartlidge RA, Nelson B, Karnezis AN, Damsky WE Jr, You MJ, DePinho RA, McMahon M, Bosenberg M. Braf(V600E) cooperates with Pten loss to induce metastatic melanoma. Nat Genet. 2009; 41:544–552. [PubMed: 19282848]

Engelhardt B, Kempe B, Merfeld-Clauss S, Laschinger M, Furie B, Wild MK, Vestweber D. P-selectin glycoprotein ligand 1 is not required for the development of experimental autoimmune

encephalomyelitis in SJL and C57BL/6 mice. J Immunol. 2005; 175:1267–1275. [PubMed: 16002731]

Frebel H, Nindl V, Schuepbach RA, Braunschweiler T, Richter K, Vogel J, Wagner CA, Loffing-Cueni D, Kurrer M, Ludewig B, Oxenius A. Programmed death 1 protects from fatal circulatory failure during systemic virus infection of mice. J Exp Med. 2012; 209:2485–2499. [PubMed: 23230000]

Gajewski TF, Schreiber H, Fu YX. Innate and adaptive immune cells in the tumor microenvironment. Nat Immunol. 2013; 14:1014–1022. [PubMed: 24048123]

Haddad W, Cooper CJ, Zhang Z, Brown JB, Zhu Y, Issekutz A, Fuss I, Lee HO, Kansas GS, Barrett TA. P-selectin and P-selectin glycoprotein ligand 1 are major determinants for Th1 cell recruitment to nonlymphoid effector sites in the intestinal lamina propria. J Exp Med. 2003; 198:369–377. [PubMed: 12885868]

Kao C, Oestreich KJ, Paley MA, Crawford A, Angelosanto JM, Ali MA, Intlekofer AM, Boss JM, Reiner SL, Weinmann AS, Wherry EJ. Transcription factor T-bet represses expression of the inhibitory receptor PD-1 and sustains virus-specific CD8+ T cell responses during chronic infection. Nat Immunol. 2011; 12:663–671. [PubMed: 21623380]

Keir ME, Butte MJ, Freeman GJ, Sharpe AH. PD-1 and its ligands in tolerance and immunity. Annu Rev Immunol. 2008; 26:677–704. [PubMed: 18173375]

Larkin J, Chiarion-Sileni V, Gonzalez R, Grob JJ, Cowey CL, Lao CD, Schadendorf D, Dummer R, Smylie M, Rutkowski P, et al. Combined Nivolumab and Ipilimumab or Monotherapy in Untreated Melanoma. N Engl J Med. 2015; 373:23–34. [PubMed: 26027431]

Ley K, Laudanna C, Cybulsky MI, Nourshargh S. Getting to the site of inflammation: the leukocyte adhesion cascade updated. Nat Rev Immunol. 2007; 7:678–689. [PubMed: 17717539]

Lin WM, Baker AC, Beroukhim R, Winckler W, Feng W, Marmion JM, Laine E, Greulich H, Tseng H, Gates C, et al. Modeling genomic diversity and tumor dependency in malignant melanoma. Cancer Res. 2008; 68:664–673. [PubMed: 18245465]

Martinez GJ, Pereira RM, Aijo T, Kim EY, Marangoni F, Pipkin ME, Togher S, Heissmeyer V, Zhang YC, Crotty S, et al. The transcription factor NFAT promotes exhaustion of activated CD8(+) T cells. Immunity. 2015; 42:265–278. [PubMed: 25680272]

Matloubian M, Concepcion RJ, Ahmed R. CD4+ T cells are required to sustain CD8+ cytotoxic T-cell responses during chronic viral infection. J Virol. 1994; 68:8056–8063. [PubMed: 7966595]

Matsumoto M, Miyasaka M, Hirata T. P-selectin glycoprotein ligand-1 negatively regulates T-cell immune responses. J Immunol. 2009; 183:7204–7211. [PubMed: 19890058]

Moskophidis D, Lechner F, Pircher H, Zinkernagel RM. Virus persistence in acutely infected immunocompetent mice by exhaustion of antiviral cytotoxic effector T cells. Nature. 1993; 362:758–761. [PubMed: 8469287]

Nakano H, Gunn MD. Gene duplications at the chemokine locus on mouse chromosome 4: multiple strain-specific haplotypes and the deletion of secondary lymphoid-organ chemokine and EBI-1 ligand chemokine genes in the plt mutation. J Immunol. 2001; 166:361–369. [PubMed: 11123313]

Paley MA, Kroy DC, Odorizzi PM, Johnnidis JB, Dolfi DV, Barnett BE, Bikoff EK, Robertson EJ, Lauer GM, Reiner SL, Wherry EJ. Progenitor and terminal subsets of CD8+ T cells cooperate to contain chronic viral infection. Science. 2012; 338:1220–1225. [PubMed: 23197535]

Pellegrini M, Calzascia T, Toe JG, Preston SP, Lin AE, Elford AR, Shahinian A, Lang PA, Lang KS, Morre M, et al. IL-7 engages multiple mechanisms to overcome chronic viral infection and limit organ pathology. Cell. 2011; 144:601–613. [PubMed: 21295337]

Petrovas C, Casazza JP, Brenchley JM, Price DA, Gostick E, Adams WC, Precopio ML, Schacker T, Roederer M, Douek DC, Koup RA. PD-1 is a regulator of virus-specific CD8+ T cell survival in HIV infection. J Exp Med. 2006; 203:2281–2292. [PubMed: 16954372]

Sabbagh L, Pulle G, Liu Y, Tsitsikov EN, Watts TH. ERK-dependent Bim modulation downstream of the 4-1BB-TRAF1 signaling axis is a critical mediator of CD8 T cell survival in vivo. J Immunol. 2008; 180:8093–8101. [PubMed: 18523273]

Sanjabi S, Mosaheb MM, Flavell RA. Opposing effects of TGF-beta and IL-15 cytokines control the number of short-lived effector CD8+ T cells. Immunity. 2009; 31:131–144. [PubMed: 19604492]

Sheppard KA, Fitz LJ, Lee JM, Benander C, George JA, Wooters J, Qiu Y, Jussif JM, Carter LL, Wood CR, Chaudhary D. PD-1 inhibits T-cell receptor induced phosphorylation of the ZAP70/CD3zeta

signalosome and downstream signaling to PKCtheta. FEBS Lett. 2004; 574:37–41. [PubMed: 15358536]

Shin H, Blackburn SD, Blattman JN, Wherry EJ. Viral antigen and extensive division maintain virus-specific CD8 T cells during chronic infection. J Exp Med. 2007; 204:941–949. [PubMed: 17420267]

Sullivan JA, Kim EH, Plisch EH, Suresh M. FOXO3 regulates the CD8 T cell response to a chronic viral infection. J Virol. 2012; 86:9025–9034. [PubMed: 22675000]

Tinoco R, Alcalde V, Yang Y, Sauer K, Zuniga EI. Cell-intrinsic transforming growth factor-beta signaling mediates virus-specific CD8+ T cell deletion and viral persistence in vivo. Immunity. 2009; 31:145–157. [PubMed: 19604493]

Topalian SL, Hodi FS, Brahmer JR, Gettinger SN, Smith DC, McDermott DF, Powderly JD, Carvajal RD, Sosman JA, Atkins MB, et al. Safety, activity, and immune correlates of anti-PD-1 antibody in cancer. N Engl J Med. 2012; 366:2443–2454. [PubMed: 22658127]

Urzainqui A, Martinez del Hoyo G, Lamana A, de la Fuente H, Barreiro O, Olazabal IM, Martin P, Wild MK, Vestweber D, Gonzalez-Amaro R, Sanchez-Madrid F. Functional role of P-selectin glycoprotein ligand 1/P-selectin interaction in the generation of tolerogenic dendritic cells. J Immunol. 2007; 179:7457–7465. [PubMed: 18025190]

Urzainqui A, Serrador JM, Viedma F, Yanez-Mo M, Rodriguez A, Corbi AL, Alonso-Lebrero JL, Luque A, Deckert M, Vazquez J, Sanchez-Madrid F. ITAM-based interaction of ERM proteins with Syk mediates signaling by the leukocyte adhesion receptor PSGL-1. Immunity. 2002; 17:401–412. [PubMed: 12387735]

Veerman KM, Carlow DA, Shanina I, Priatel JJ, Horwitz MS, Ziltener HJ. PSGL-1 regulates the migration and proliferation of CD8(+) T cells under homeostatic conditions. J Immunol. 2012; 188:1638–1646. [PubMed: 22250093]

Veerman KM, Williams MJ, Uchimura K, Singer MS, Merzaban JS, Naus S, Carlow DA, Owen P, Rivera-Nieves J, Rosen SD, Ziltener HJ. Interaction of the selectin ligand PSGL-1 with chemokines CCL21 and CCL19 facilitates efficient homing of T cells to secondary lymphoid organs. Nat Immunol. 2007; 8:532–539. [PubMed: 17401367]

Virgin HW, Wherry EJ, Ahmed R. Redefining chronic viral infection. Cell. 2009; 138:30–50. [PubMed: 19596234]

West EE, Jin HT, Rasheed AU, Penaloza-Macmaster P, Ha SJ, Tan WG, Youngblood B, Freeman GJ, Smith KA, Ahmed R. PD-L1 blockade synergizes with IL-2 therapy in reinvigorating exhausted T cells. J Clin Invest. 2013; 123:2604–2615. [PubMed: 23676462]

Wherry EJ. T cell exhaustion. Nat Immunol. 2011; 12:492–499. [PubMed: 21739672]

Wherry EJ, Blattman JN, Murali-Krishna K, van der Most R, Ahmed R. Viral persistence alters CD8 T-cell immunodominance and tissue distribution and results in distinct stages of functional impairment. J Virol. 2003; 77:4911–4927. [PubMed: 12663797]

Wolchok JD, Kluger H, Callahan MK, Postow MA, Rizvi NA, Lesokhin AM, Segal NH, Ariyan CE, Gordon RA, Reed K, et al. Nivolumab plus ipilimumab in advanced melanoma. N Engl J Med. 2013; 369:122–133. [PubMed: 23724867]

Zajac AJ, Blattman JN, Murali-Krishna K, Sourdive DJ, Suresh M, Altman JD, Ahmed R. Viral immune evasion due to persistence of activated T cells without effector function. J Exp Med. 1998; 188:2205–2213. [PubMed: 9858507]

Zarbock A, Muller H, Kuwano Y, Ley K. PSGL-1-dependent myeloid leukocyte activation. J Leukoc Biol. 2009; 86:1119–1124. [PubMed: 19703898]

Zinselmeyer BH, Heydari S, Sacristan C, Nayak D, Cammer M, Herz J, Cheng X, Davis SJ, Dustin ML, McGavern DB. PD-1 promotes immune exhaustion by inducing antiviral T cell motility paralysis. J Exp Med. 2013; 210:757–774. [PubMed: 23530125]

Highlights

- T cell survival was increased in *Selplg*$^{-/-}$ mice after chronic virus infection
- Multi-functional anti-viral T cells in *Selplg*$^{-/-}$ mice promoted viral control
- Ligating PSGL-1 on exhausted CD8^{+} T cells silenced TCR signals
- PSGL-1-deficiency enhanced T cell anti-tumor immunity to melanoma

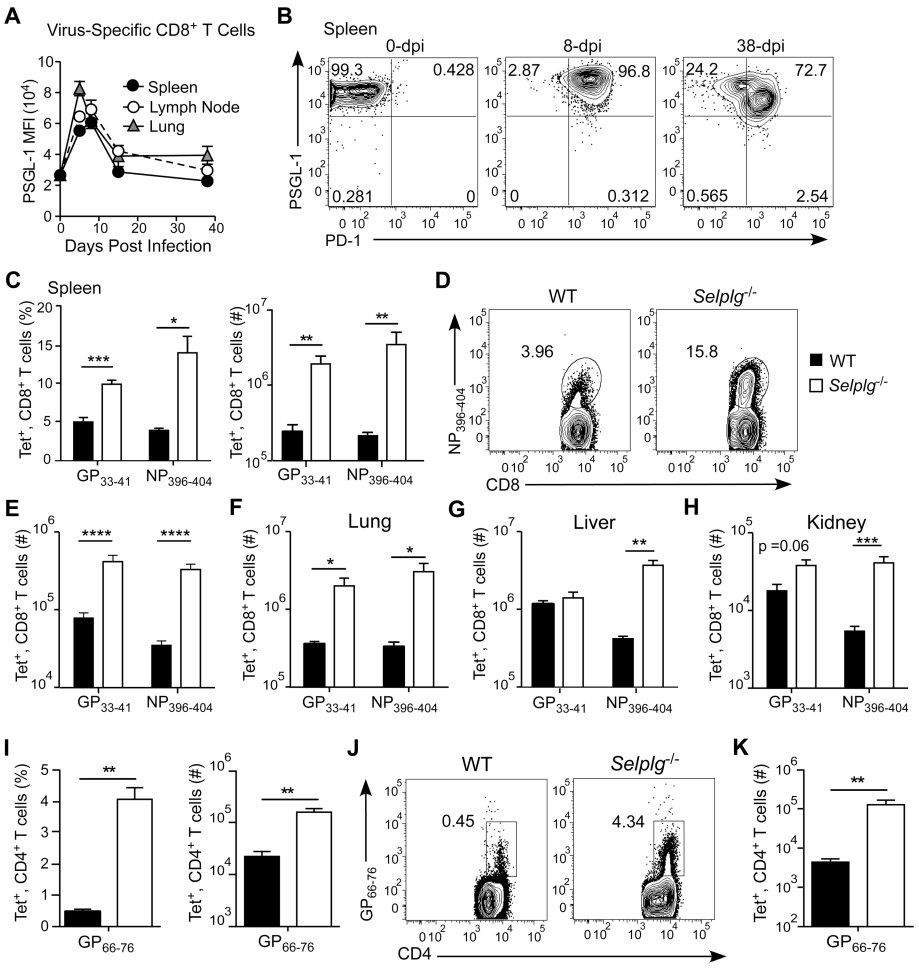

Figure 1. PSGL-1 kinetics and accumulation of virus-specific T cells in *Selplg*$^{-/-}$ mice after LCMV Clone 13 infection

WT and *Selplg*$^{-/-}$ mice were infected with 2 × 10^6 PFU LCMV Cl13. (**A**) WT mice were injected with P14 T cells and the mean fluorescence intensity (MFI) of PSGL-1 on P14 CD8$^+$ T cells from spleen, lymph nodes, lung was analyzed, (**B**) with representative flow cytometry plots from spleen. (**C**) Virus-specific CD8$^+$ T cell frequencies and numbers in the spleens of WT and *Selplg*$^{-/-}$ mice at 8-dpi, (**D**) with representative flow cytometry plots (**D**) and (**E**) numbers at 30-dpi. Numbers of tetramer$^+$ CD8$^+$ T cells in lung (**F**), liver (**G**), and kidney (**H**) at 10-dpi. (**I**) Frequencies and numbers of $GP_{66-76}$$^+$ CD4$^+$ T cells in spleen at 8-dpi with representative flow cytometry plots in (**J**) and numbers in lung (**K**). Data are representative of 3 independent experiments with ≥ 5 per group. See also Figures S1, S2.

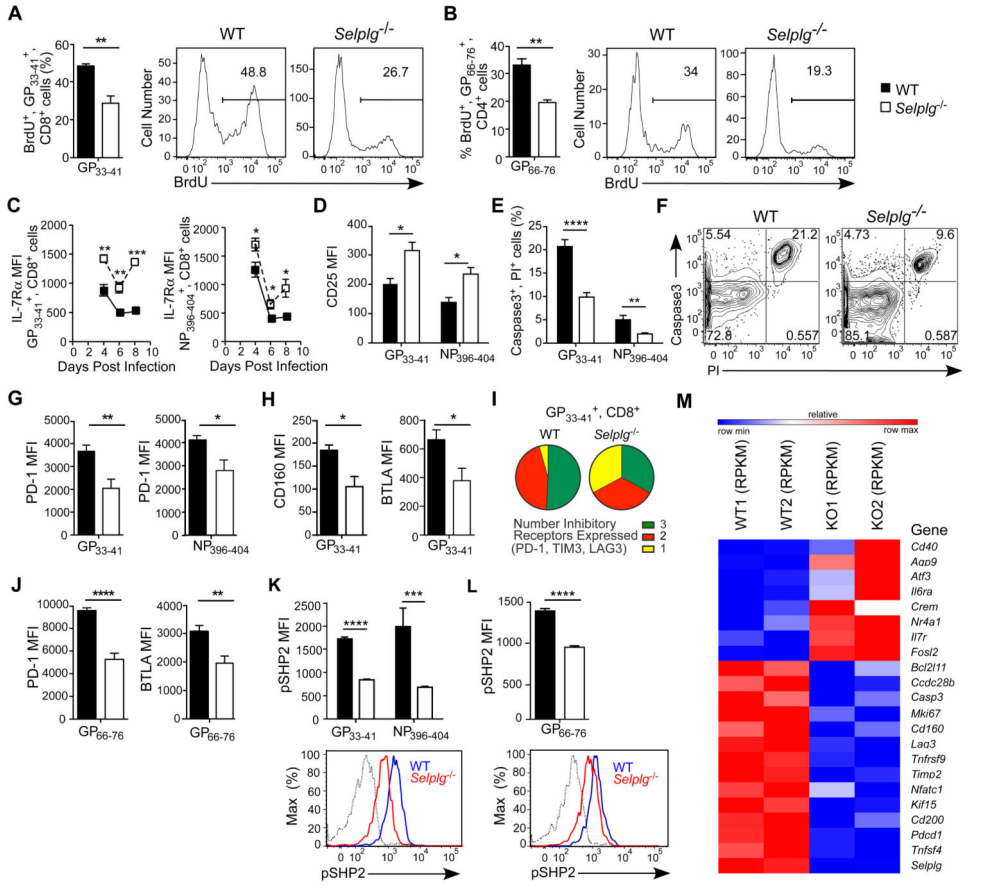

Figure 2. Virus-Specific *Selplg*$^{-/-}$ T cells display enhanced survival and reduced inhibitory receptor expression

BrdU uptake by $GP_{33\text{-}41}^{+}$ $CD8^{+}$ T cells **(A)** and $GP_{66\text{-}76}^{+}$ $CD4^{+}$ T cells (**B**) at 9-dpi in spleen. Mean fluorescence intensity (MFI) of (**C**) IL-7Rα and (**D**) CD25 in blood on tetramer^{+} $CD8^{+}$ T cells. (**E,F**) Caspase3 and PI staining at 10-dpi. (**G,H**) PD-1, CD160, and BTLA MFI on tetramer^{+} $CD8^{+}$ T cells at 9-dpi in the spleen. (**I**) The number of inhibitory receptors expressed on $GP_{33\text{-}41}^{+}CD8^{+}$ cells from spleen at 10dpi using boolean gating (**J**). PD-1 and BTLA MFI on $GP_{66\text{-}76}^{+}$ $CD4^{+}$ T cells 8-dpi from spleen. Phospho-SHP2 (pSHP2) in (**K**) $CD8^{+}$ $GP_{33\text{-}41}^{+}$ and (**L**) $CD4^{+}$ $GP_{66\text{-}76}^{+}$ cells at 10dpi. (**M**) Heat map showing expression of selected genes from WT or *Selplg*$^{-/-}$ $GP_{33\text{-}41}^{+}$ $CD8^{+}$ T cells FACS sorted from spleen at 9-dpi. Data are representative of 3 independent experiments with ≥ 5 mice per group. See also Figure S2, S3.

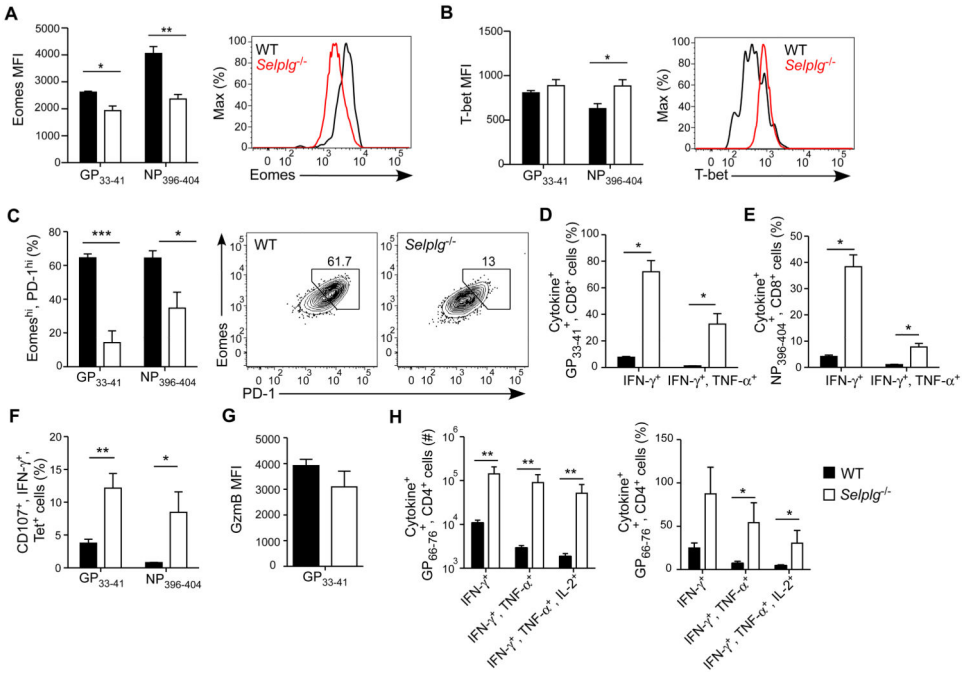

Figure 3. Enhanced effector T cell function in *Selplg*$^{-/-}$ mice

(**A**-**H**). Expession of Eomes (**A**) and T-bet (**B**) or both (**C**) by GP-$_{33\text{-}41}^{+}$ and NP$_{396\text{-}404}^{+}$ CD8^{+} cells and by GP$_{66\text{-}76+}$ CD4^{+} cells from Cl13 infected mice at 10-dpi. The spleen cells were stimulated with LCMV peptides and assayed for IFN-γ, TNF-α, and IL-2 production by CD8^{+} T cells (**D**-**E**) or CD4^{+} T cells (**H**). (**F**) Tetramer^{+} CD8^{+} T cell function measured by IFN-γ and CD107 staining. (**G**) Mean fluorescence intensity (MFI) of Granzyme B expression in tetramer^{+} CD8^{+} T cells. Cytokine production on a per cell basis (**D,E,H**) was determined by normalizing the number of cytokine-producing cells to the number of tetramer^{+} cells for each LCMV peptide. Data are representative of 3 independent experiments with ≥ 5 mice per group. See also Figure S4, S5.

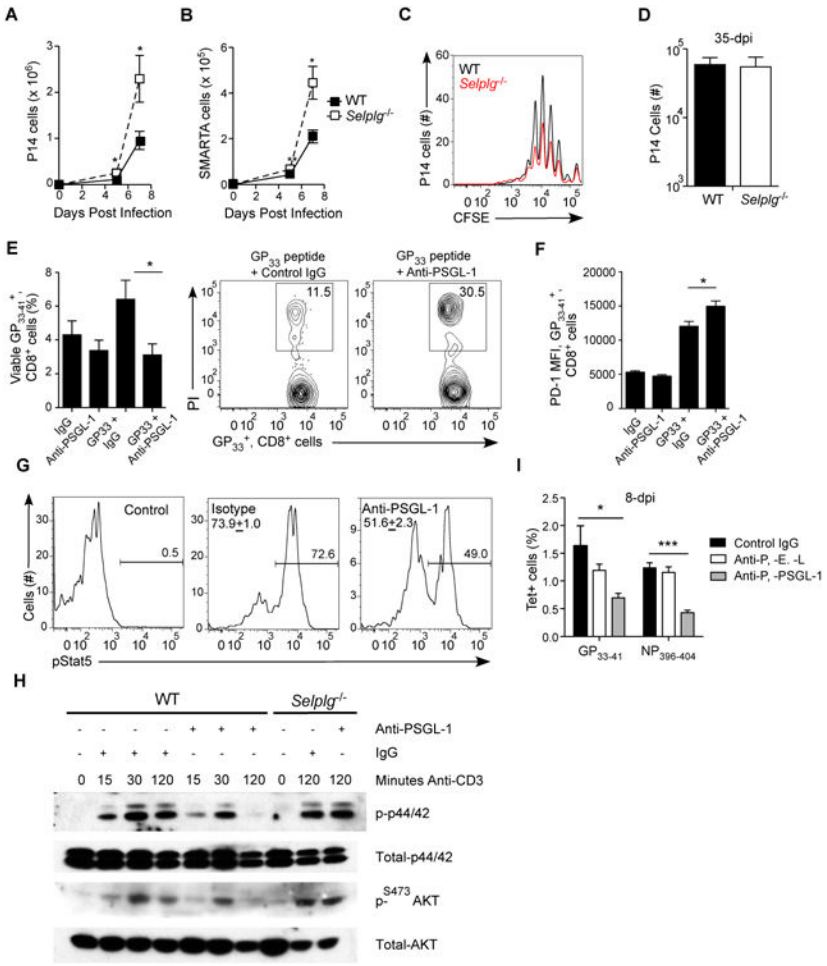

Figure 4. PSGL-1 ligation of exhausted CD8$^+$ T cells silences IL-2 and TCR signaling diminishing their survival

WT and *Selplg*$^{-/-}$ naïve P14 CD8$^+$ T cells 1:1 (10^3 cells) or *Selplg*$^{-/-}$ naïve SMARTA transgenic CD4$^+$ T cells 1:1 (10^3 cells) were cotransferred i.v. into WT mice that were infected 1 day later with Cl13. The number of WT and *Selplg*$^{-/-}$ P14 cells (**A**) or SMARTA cells (**B**) in spleen on the indicated days. (**C**) CFSE dilution by WT or *Selplg*$^{-/-}$ P14 cells at 2-dpi. (**D**) Number of P14 cells at 35-dpi. The frequency of live (PI$^-$) GP$_{33\text{-}41}{}^+$ CD8$^+$ T cells (**E**) and their expression of PD-1 (**F**) after culture for 4 days in the absence (control) or presence of GP$_{33\text{-}41}$ and either with anti-PSGL-1 or control Ig. (**G**) The frequency of pSTAT-5$^+$ GP$_{33\text{-}41}{}^+$ CD8$^+$ T cells. (**H**). Immunoblot of WT CD8$^+$ T cells FACS sorted at 8-dpi and stimulated with anti-CD3 for the indicated times, (**I**) Frequency of tetramer$^+$ cells in blood at 8-dpi after injection of the indicated antibodies. Data are representative of 3 (**A-G**) or 2 (**H,I**) independent experiments, with ≥ 5 mice per group. See also Figure S6.

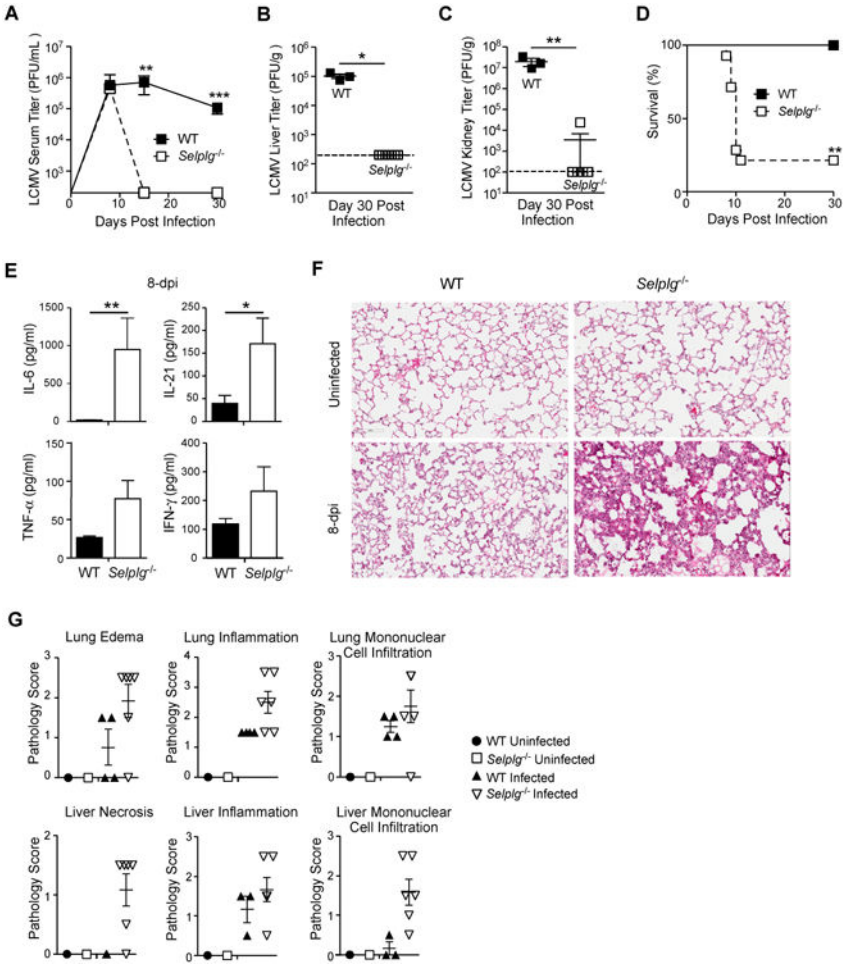

Figure 5.

***Selplg*$^{-/-}$ mice have accelerated viral control and extensive immunopathology.** Virus in serum (**A**), liver (**B**), kidney (**C**), survival curves (**D**), and serum cytokine concentrations (pg/mL) at 8-dpi with Cl13 (**E**). (**F**) Representative histology of lungs from WT and *Selplg*$^{-/-}$ mice without infection and at 8-dpi. (**G**) Pathology scores of lungs and livers. Viral titers in (**A**) are pooled data from 3 independent experiments. Data are representative of 3 (**A-D**) or 2 (**E-G**) independent experiments with ≥ 3 mice per group).

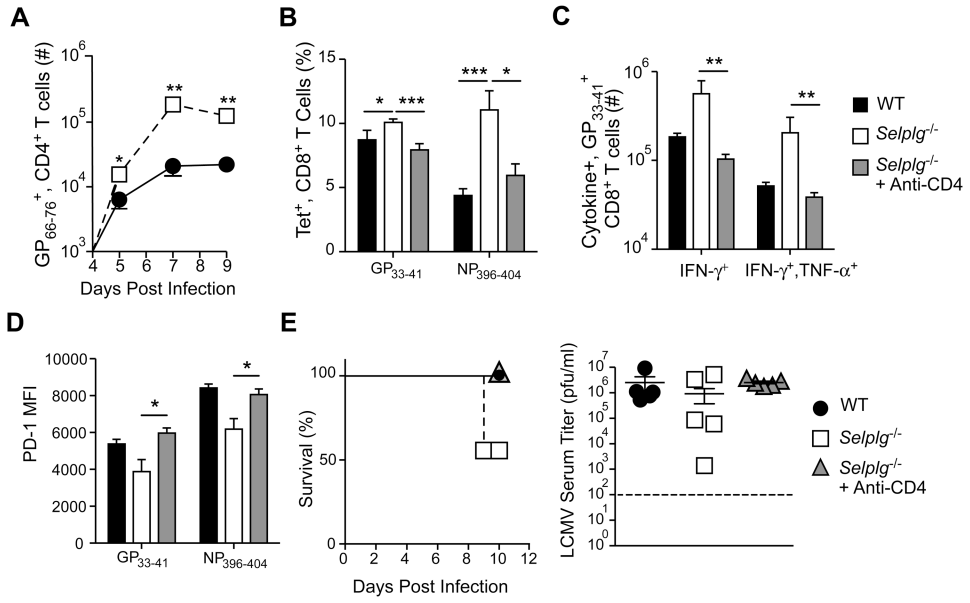

Figure 6. Optimal virus-specific CD8$^+$ T cell function in *Selplg*$^{-/-}$ mice depends on CD4+ T cell help

(**A**) Numbers of $GP_{66\text{-}76}{}^+$ $CD4^+$ T cells in the spleen after Cl13 infection. (**B-E**) WT, *Selplg*$^{-/-}$, and *Selplg*$^{-/-}$ depleted of $CD4^+$ T cells by antibody treatment were infected with Cl13. (**B**) Frequencies of tetramer$^+$ $CD8^+$ T cells in blood at 8-dpi. (**C**) Number of cytokine producing $GP_{33\text{-}41}{}^+$ $CD8^+$ T cells in spleen at 10-dpi. (**D**) Mean fluorescence intensity (MFI) of PD-1 on tetramer$^+$ $CD8^+$ T cells in spleen at 10-dpi. (**E**) Survival and serum virus concentrations at 10-dpi. Data are representative of 3 independent experiments with ≥ 5 mice per group.

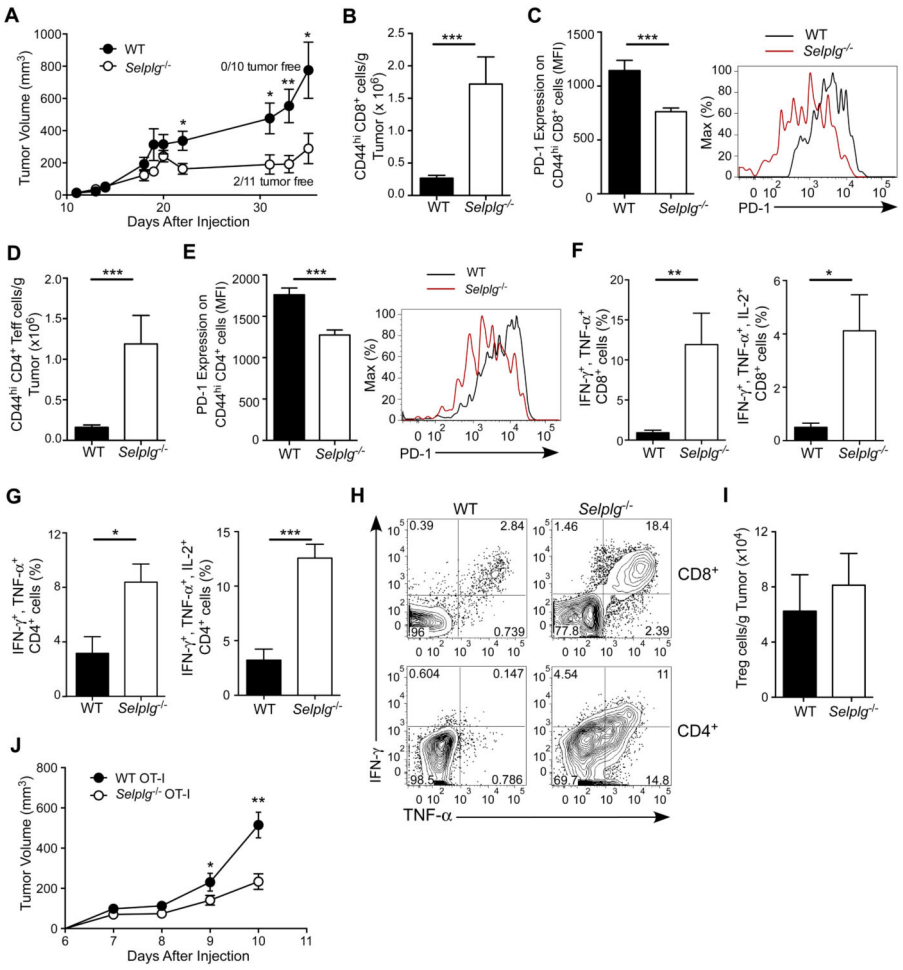

Figure 7. Enhanced anti-tumor T cell responses in *Selplg*$^{-/-}$ mice

(**A-I**) WT and *Selplg*$^{-/-}$ mice received Yumm1.5 melanoma cells by s.c. injection. (**A**) Tumor volumes with time post-injection. (**B**) Numbers of effector (CD44^{hi}) CD8^{+} T cells/g of tumor and (**C**) PD-1 expression. (**D**) Numbers of effector (CD44^{hi}) CD4^{+} T cells/g of tumor and (**E**) PD-1 expression. Cytokine production by tumor-infiltrating CD8^{+} (**F**) and CD4^{+} T cells (**G**) and (**H**) representative flow cytometry plots. (**I**) Numbers of Treg cells/g of tumor. (**J**) WT mice were injected s.c. with B16-OVA melanoma cells and 7 days later were injected i.v. with effector WT OT-I or *Selplg*$^{-/-}$ OT-I T cells; afterwards tumor growth was analyzed. Data are representative of 3 or 2 (**J**) independent experiments with ≥ 5 mice per group. See also Figure S7.